47th AIAA/ASME/ASCE/AHS/ASC Structures, Structural Dynamics, and Materials Con
1-4 May 2006, Newport, Rhode Island

AIAA 2006-1962

Failure Analysis of Adhesively Bonded Composite Joints via the Virtual Crack Closure Technique

Phillip W. Yarrington* and Craig S. Collier†
Collier Research Corp., Hampton, VA 23666

Brett A. Bednarcyk‡
Ohio Aerospace Institute, Cleveland, OH 44142

Failure analysis of bonded composite joints is essential to the design of modern aerospace vehicles where adhesive joints are widely used. Recently, methods for stress and failure analysis of composite bonded joints were implemented within the HyperSizer® stiffened panel design/analysis/optimization software package. The capability uses efficient, non-finite element based methods to calculate the adhesive stresses and detailed in-plane and out-of-plane interlaminar shear and peel stresses in the adherends for predicting damage initiation and failure. Previously, HyperSizer predicted failure using 19 different leading ply and interlaminar stress/strain-based fracture and delamination bonded joint failure theories. Now, the joint failure analysis capability has been extended to include damage tolerance residual strength by using the virtual crack closure technique (VCCT), which predicts the growth of an existing crack by comparing calculated strain energy release rates to critical values determined from tests. Implementation of VCCT, specific to the HyperSizer joint analysis method, is discussed and results are compared to finite element analysis and experimental results from the literature for composite and isotropic joint adherends.

I. Introduction

Methods for stress and failure analysis of composite bonded joints have recently been developed and implemented in the HyperSizer® stiffened structural sizing software package[1-5]. This new capability to calculate accurate three-dimensional stresses enables prediction of failure loads in bonded composite joints with complex 3D stress states. Failure prediction requires not only accurate stress analysis, but also use of appropriate failure criteria associated with specific failure modes. For bonded joints, the failure occurs either within the adhesive (cohesive failure), at the adhesive/adherend interface (interface failure), or in the adherends. Metallic adherends generally fail in relatively simple modes compared to composite adherends, which may fail in matrix tension/compression, fiber tension/compression, delamination, etc. In some cases, composite joints fail progressively after damage is initiated in the adherends or in the adhesive. The ultimate failure of a joint will then not be reached until the progressively accumulated damage exceeds some tolerance. The process of damage growth is relatively complex and not easy to predict using conventional material strength methodologies. Interfacial failure is particularly complex because of the formation of chemical bonds, whose strengths are difficult to measure. As such, HyperSizer's joint analysis methods have been extended to include the virtual crack closure technique

* Senior Research Engineer, phil.yarrington@hypersizer.com, AIAA Member.
† Senior Research Engineer, craig.collier@hypersizer.com, AIAA Senior Member.
‡ Senior Scientist, 22800 Cedar Point Rd., Cleveland, OH 44142, bednarcyk@oai.org, AIAA Member.

(VCCT)[6,7], which considers a joint with an existing crack and attempts to predict whether crack growth will occur. This method is based on strain energy release rate (SERR) rather than critical stress and is thus less sensitive to stress concentrations/singularities that can arise in joint analyses. VCCT has been employed in the past predominantly in the context of finite element analysis (FEA), but herein, the method is adapted to the non-FEA HyperSizer joint analysis techniques.

The purpose of this paper is to describe the implementation of VCCT within the HyperSizer joint analysis methods and to compare HyperSizer VCCT predictions with those from the literature for validation and verification. Comparisons are presented for bonded doubler, double cantilever beam (DCB), and mixed mode bending (MMB) configurations with both isotropic and composite constituent materials. The results indicate good agreement between HyperSizer and the models and experiments presented in the literature. In addition, issues related to analysis point spacing/convergence and cohesive region stiffness are investigated and discussed.

II. Description of HyperSizer Joint Analysis Method

HyperSizer's bonded joint stress analysis method was developed based upon Mortensen's unified approach[8,9], but it has been extended considerably and modified to enable accommodation of transverse in-plane straining, hygrothermal loads, computation of the local in-plane and interlaminar stresses throughout the adherends, and accommodation of pressure loading[1-5]. Compared to other analytical (i.e., non-FEA) methods used for bonded joint analysis, the HyperSizer method is capable of handling more general situations, including various joint geometries, asymmetric and unbalanced laminates, and more general loading and boundary conditions. A wide range of joint types may be considered, and the adherends, which were originally modeled as classical laminates in cylindrical bending, are now considered to undergo 'generalized cylindrical bending', in which transverse straining is accommodated. Both linear and nonlinear behavior of an adhesive layer is admitted in the analysis. For linear analysis, the adhesive layer is modeled via a traction-separation law that responds similarly to the linear behavior cohesive elements within the ABAQUS finite element software[10,11]. This can be used to simulate a physical adhesive layer present in the joint, or, for cases without a non-negligible adhesive layer, the traction-separation model represents a zero-thickness cohesive layer that can be given a high penalty stiffness to hold the adherends together[11,12]. Inclusion of nonlinear adhesive behavior in the analysis is accomplished through the use of a secant modulus approach for the nonlinear tensile stress–strain relationship in conjunction with a yield criterion.

The equilibrium equations for each joint type are derived through direct imposition of force and moment equilibrium on joint elements, and by combination of the aforementioned equations and relations, a set of governing ordinary differential equations is obtained. The governing system of equations is solved numerically using Mortensen and Thomsen's[9] 'multi-segment method of integration,' yielding laminate-level fields and adhesive stresses that vary along the joint in each adherend. After the governing equations are solved, the ply-level in-plane stress components in the adherends can be calculated from Classical Lamination Theory (CLT). After solving for the in-plane stresses, the interlaminar stress components in the adherends are obtained through integration of the point-wise equilibrium equations. The details of HyperSizer's stress analysis method are described by Zhang et al.[2]. It is important to recognize that the HyperSizer joint analysis method is very efficient; the execution time for a typical problem is approximately 1/40 second. Furthermore, problem set up and post-processing is straightforward, enabling rapid consideration of a wide range of joint configurations for sizing optimization.

III. VCCT Implementation

The Virtual Crack Closure Technique (VCCT)[7], originally proposed by Rybicki and Kanninen[6], has gained popularity in recent years as it provides an effective means to predict the onset of crack growth by

calculating the strain energy release rate associated with a crack. It has typically been implemented within the finite element method, where it overcomes typical FEA problems with stress singularities at the crack tip and the associated extreme mesh dependence. VCCT has now been implemented within HyperSizer's analytical (non-FEA) joint analysis methods. This has enabled rapid design/analysis/sizing of bonded joints for damage tolerance.

Implementation of VCCT within a two-dimensional finite element model is depicted in Fig. 1[6]. Three-dimensional solid model and shell generalizations are also presented by Krueger[6] and are fairly straightforward. A pre-existing crack is explicitly included in the finite element mesh. The key assumption is that the energy released by extending the crack by length Δa is equal to the work required to close the crack over the length Δa. It is further assumed, as shown in Fig. 1, that if the crack is extended by an additional length increment of Δa, the state at the new crack tip remains the same as does the energy released. If, as shown in Fig. 1, the element length is equal to Δa, the force required to close the crack along the last element at the crack tip is equal to the nodal force at the crack tip. Under the above assumptions, the strain energy release rate (SERR) is calculated from the nodal forces at the crack tip along with the nodal displacements directly before the crack tip. For the 2D case shown in Fig. 1, the mode I (opening) and mode II (in-plane shear) SERRs can be written as,

$$G_I = -Z_i \frac{(w_\ell - w_{\ell^*})}{2\,\Delta a} \tag{1}$$

$$G_{II} = -X_i \frac{(u_\ell - u_{\ell^*})}{2\,\Delta a} \tag{2}$$

where Z_i and X_i are the nodal force components at the crack tip (node i) and w_ℓ, w_{ℓ^*}, u_ℓ, and u_{ℓ^*} are the nodal displacements shown at nodes ℓ and ℓ^*.

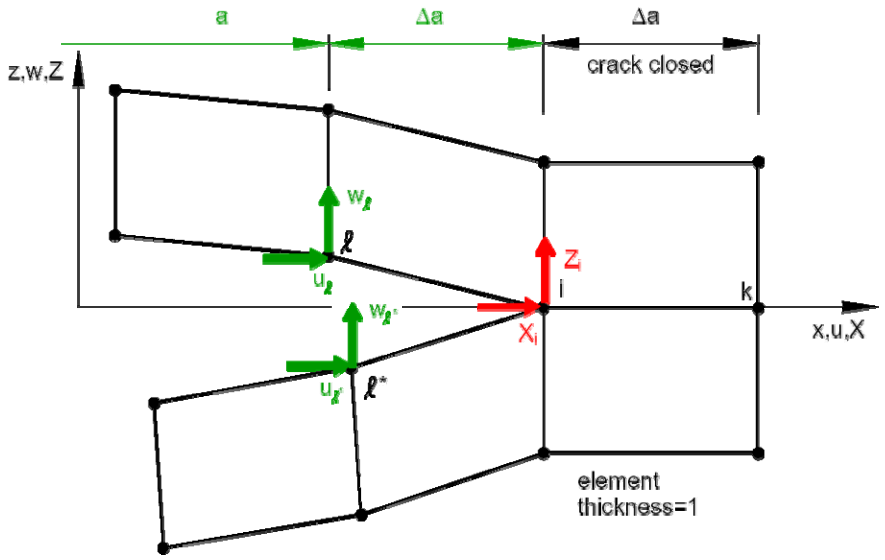

Fig. 1 Implementation of VCCT within the finite element method, after Krueger[6].

In HyperSizer, the SERR is calculated in a manner similar to that employed in FEA. The crack is introduced by effectively eliminating cohesion of the adherends in the desired cracked region, as illustrated in Fig. 2. The cohesion is modeled via a traction-separation law that has no physical thickness within the HyperSizer joint analysis method. When an adhesive is present in the simulated joint, the cohesive region represents the adhesive material, and its properties are determined from the adhesive material properties and thickness. When no such adhesive material is present, the cohesive region is provided a high penalty stiffness that holds the adherends together ahead of the crack.

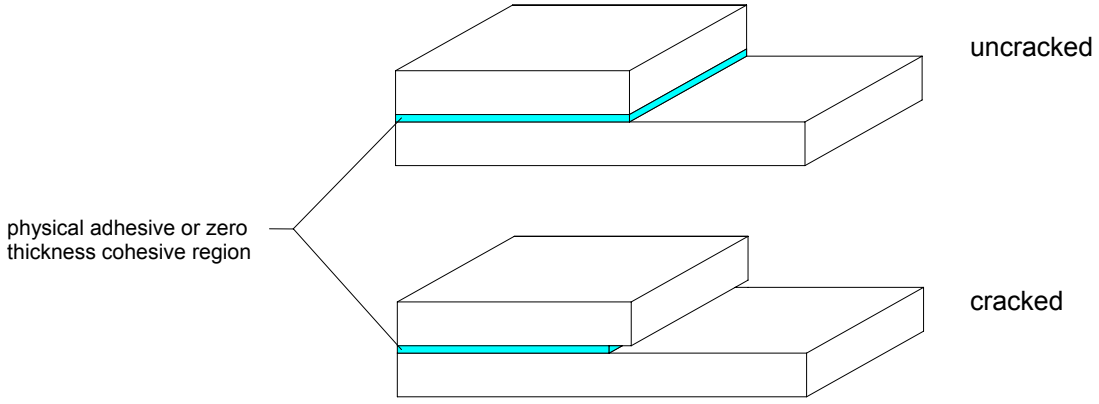

Fig. 2 A delamination crack is introduced into the HyperSizer joint model by effectively removing the cohesion in the cracked region.

The HyperSizer joints analysis method employs a number of analysis points along the joint (at which the solution to the governing differential equations is determined) and through the adherend thickness (at which the ply in-plane and interlaminar stresses are determined). Figure 3 shows the analysis points along the adherend interfaces for a case in which a crack has been introduced. The adherends are labeled "T" for top and "B" for bottom. In the detail of the crack tip, the analysis points at and on either side of the crack tip have been labeled "1", "2", and "3", with point 2 representing the crack tip. The force components at the crack tip are denoted as X and Z. By considering crack extension to be the length between two analysis points, Δa, the SERR can be calculated from the crack tip forces and the relative displacements of the adherends at analysis point 3. That is,

$$G_I = \frac{Z\left[w_T(3) - w_B(3)\right]}{2\Delta a} \tag{3}$$

$$G_{II} = \frac{X\left[u_T(3) - u_B(3)\right]}{2\Delta a} \tag{4}$$

$$G_{III} = \frac{Y\left[v_T(3) - v_B(3)\right]}{2\Delta a} \tag{5}$$

where $u_T(3)$, $u_B(3)$, $w_T(3)$, $w_B(3)$, $v_T(3)$, and $v_B(3)$ are the displacement components at analysis point 3 (see Fig. 3). The total SERR can then be calculated as,

$$G_T = G_I + G_{II} + G_{III} \tag{6}$$

Note that, for clarity of Fig. 3, the third crack tip force component (Y) and the y-direction displacements (v) were omitted although these terms do arise with HyperSizer joint analysis in the general case. The adhesive force components and adherend interfacial displacements needed to determine the mixed mode SERR values in equations (3 – 5) are easily extracted from the adhesive layer tractions at points 1, 2, and 3 with no computational price. The HyperSizer joint analysis implementation of the VCCT method thus represents a new application of VCCT in a non-FEA, rapid analysis. It enables quick consideration of thousands of potential joint configurations and load levels in the context of VCCT during preliminary trade studies.

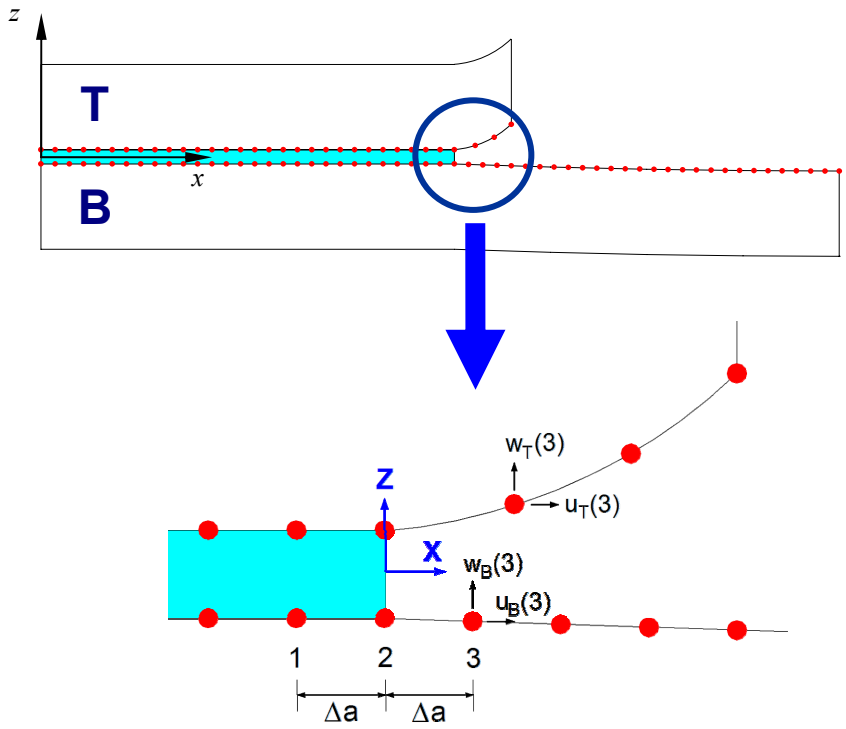

Fig. 3 Details of the HyperSizer joint analysis VCCT implementation. Similar to the FEA implementation of VCCT, HyperSizer calculates SERRs based on the normal and tangential forces at the crack tip (location 2) and the relative normal and tangential displacements in the separated region (location 3).

IV. Validation Examples

A. Bonded Doubler Example

This example problem was analyzed by Wang et al.[13] and Raju et al.[14] using shell, plane strain, and three-dimensional solid FEA models. The bonded doubler analysis geometry considered, shown in Fig. 4, was intended to represent a stiffener flange bonded to a skin. The dimensions are: l_1 = 1 in., l_2 = 1 in., b = 1 in., a = 0.4 in., h = 0.0875 in. The adherends consist of unidirectional graphite/epoxy composites oriented in the x-direction with material properties: E_1 = 19.5 Msi, E_2 = 1.48 Msi, G_{12} = 0.8 Msi, ν_{12} = 0.3. The simulated loading involves a shear force resultant, Q = 60 lb/in. In the finite element analyses, no

cohesive region exists between the adherends; rather, the uncracked area of the adherend interface is considered to be perfectly bonded and continuous. As discussed in Section III, cohesion in the HyperSizer joint analysis method is enforced via a traction-separation law that holds the adherends together in the uncracked region. The stiffnesses that relate the tractions to the separations of the cohesive region (termed "penalty stiffnesses" by Comanho and Davila[11]), in the case of a physical adhesive layer, are given by,

$$K_p^I = E_a / t_a \tag{7}$$

$$K_p^{II} = K_p^{III} = G_a / t_a \tag{8}$$

where, K_p^I, K_p^{II}, and K_p^{III} are the mode I, II, and III penalty stiffnesses, E_a and G_a are the adhesive elastic and shear moduli, and t_a is the adhesive thickness. In the present bonded doubler example, there is no physical adhesive, thus the penalty stiffness must be chosen rather than calculated from adhesive properties. Three cases were considered, with low, moderate, and high penalty stiffnesses, as summarized in Table 1.

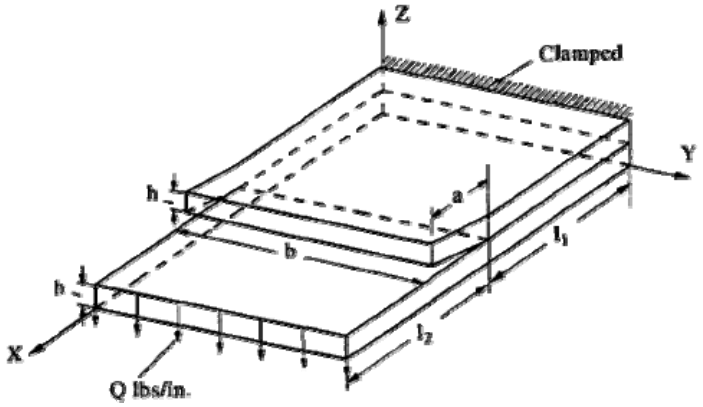

Fig. 4. Bonded doubler geometry considered by Wang et al.[13] and Raju et al.[14] via FEA, after Raju et al.[14]

Table 1 Cohesive region penalty stiffness values considered for the bonded doubler.

	Cohesive Region Stiffness		
	Low	Moderate	High
K_p^I ($\times 10^6$ lb/in^3)	111	1,110	25,000
K_p^{II} ($\times 10^6$ lb/in^3)	41	410	9,615

Figure 5 shows a plot of the cohesive peel stress predicted by HyperSizer between the joint adherends leading up to the crack tip as a function of the cohesive penalty stiffness. The crack tip stress profiles shown, which exhibit high but non-singular concentrations, are typical of the HyperSizer joint analysis method. Most notable in Fig. 5 is the strong dependence of the concentration magnitude on the penalty stiffness. Table 2 lists the magnitudes of the cohesive peel and shear stress concentrations, along with the

total SERR predicted by HyperSizer for the bonded doubler problem. This table illustrates that, while there is a strong dependence of the concentration on the penalty stiffness value, the total SERR exhibits only a weak dependence. In particular, comparing the low and high penalty stiffness cases, there is change of more than 1300% in the stress concentrations, while there is only a 9.6% change in calculated SERR. Obviously, examining equations (3 – 5), when the penalty stiffness rises, so too does the nodal force at the crack tip, which tends to increase the SERR values. However, an increased penalty stiffness also tends to decrease the relative nodal displacements, which then lowers the calculated SERR values.

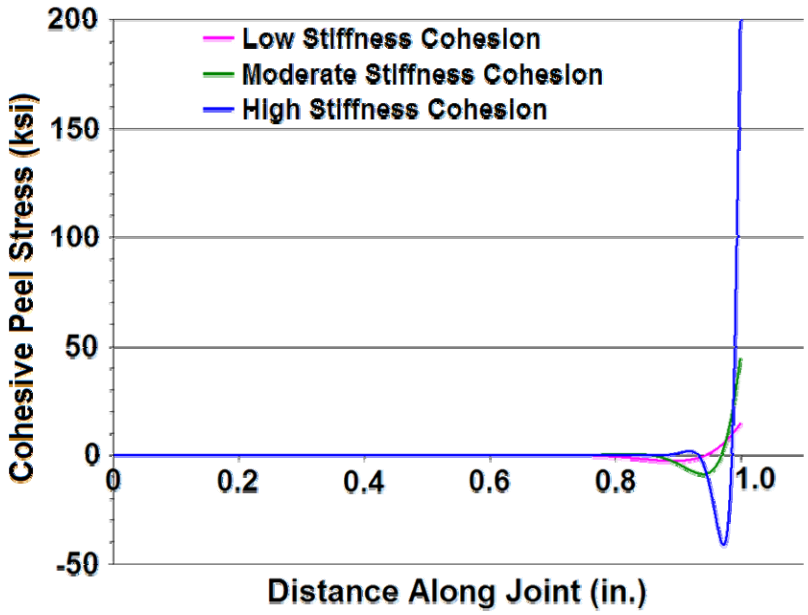

Fig. 5 Predicted peel stress in the cohesive region between the adherends of the bonded doubler joint as a function of penalty stiffness. The distance along the joint of 1.0 in. corresponds to the location of the crack tip.

Table 2 HyperSizer predictions for the maximum cohesive peel and shear stresses and the total SERR as a function of cohesive penalty stiffness.

	Max. Peel Stress (ksi)	Max Shear Stress σ_{yz} (ksi)	Total SERR (in-lb/in^2)
Low Penalty Stiffness	14.4	7.51	1.638
Moderate Penalty Stiffness	44.3	23.0	1.54
High Penalty Stiffness	203	109	1.48

Another important issue to consider with respect to the HyperSizer SERR predictions is the effect of the analysis point spacing at the crack tip. As shown in Fig. 3, the HyperSizer joint analysis method employs a number of analysis points along the joint at which the solution to the governing system of differential equations is determined. The point-wise results in the vicinity of the crack tip are then used to determine the SERR values for the different modes. Fig. 6 illustrates the convergence of the mode I, mode II, and total SERR predicted by HyperSizer for the bonded doubler problem. The lines with symbols appearing in Fig. 6 represent the low penalty stiffness predictions as a function of the analysis point spacing at the crack tip. It appears that convergence has been achieved for an analysis point spacing

of 0.001 in. Note that the analysis point spacing within the HyperSizer joint analysis method can be varied along the joint, so a fine analysis point spacing may be employed locally near the crack tip while maintaining maximum efficiency by utilizing a coarse analysis point spacing elsewhere.

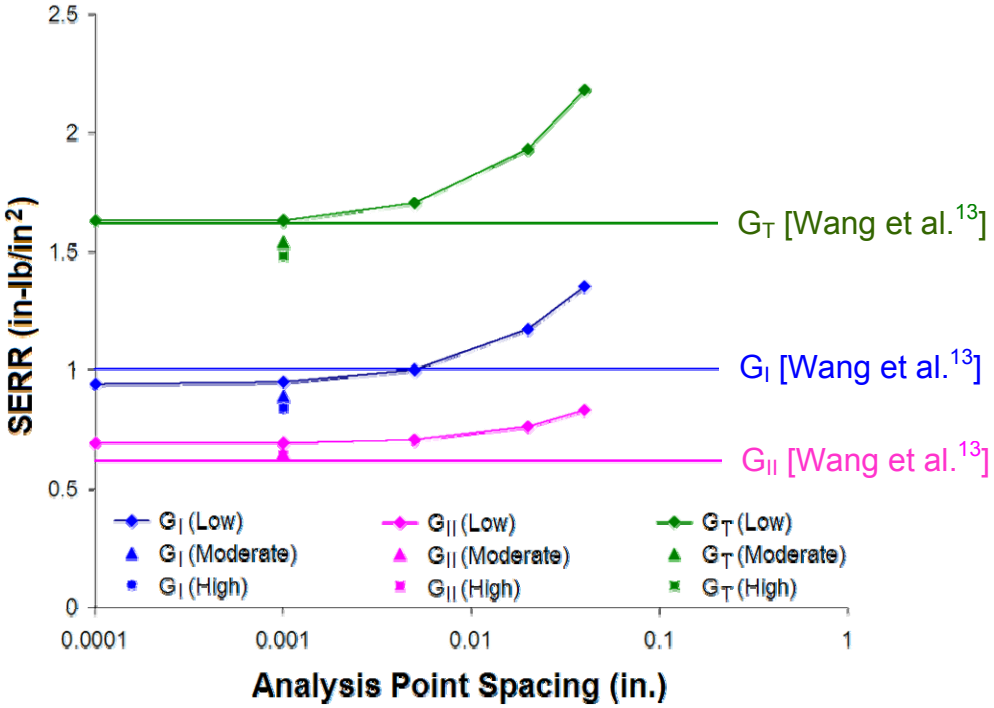

Fig. 6 SERR predicted by HyperSizer as a function of analysis point spacing at the crack tip. The mode I (G_I), mode II (G_{II}) and total (G_T) SERR values are compared to the shell FEA results of Wang et al.[13]

Also plotted in Fig. 6 are the predicted SERR values for intermediate and high cohesive penalty stiffnesses with an analysis point spacing of 0.001 in., along with the shell FEA SERR predictions of Wang et al.[13] Comparison of the HyperSizer results to the results of Wang et al. [13] and Raju et al.[14] are also presented in Table 3. Because the HyperSizer joint analysis method treats the joint adherends as plates, the most appropriate comparison of the HyperSizer results is with the shell FEA results of Wang et al.[13], however it is interesting to note the variability in the FEA results as a function of element type and, in the case of the 3D solid analysis, mesh refinement. Figure 5 and Table 3 indicate that HyperSizer tends to under predict the G_I value and over predict the G_{II} value slightly compared to the FEA results from the literature. The HyperSizer results that employed the low penalty stiffness provide the best match to the shell FEA results, with a G_T that differs by only 2.5%. Turon et al.[15] address the issue of the cohesive penalty stiffness in the context of FEA cohesive delamination analyses. These authors express the mode I penalty stiffness as,

$$K_p^I = \frac{\alpha E_3}{t} \tag{9}$$

where E_3 is the through-thickness elastic modulus of the adherend material ($E_2 = E_3$ for transversely isotropic materials), t is the adherend thickness, and α is a parameter that should be chosen to be much

larger than 1 in order for the joint to be unaffected by the cohesive surface. For the bonded doubler problem considered herein, the low, moderate, and high penalty stiffness values correspond to α values of 6.57, 65.7, and 1480. Davila[10] recommended an α value of 50, which would suggest that the HyperSizer bonded doubler SERR predictions with the intermediate penalty stiffness are the most appropriate. However, fully understanding the relationship between the analytical (non-FEA) HyperSizer SERR predictions and the cohesive penalty stiffness requires additional study.

Table 3 Comparison of HyperSizer predictions of the bonded doubler problem SERR values with FEA results from the literature.

		SERR (in-lb/in^2)		
		G_I	G_{II}	G_T
3D Solid FEA[14]	Coarse Mesh	0.987	0.597	1.584
	Fine Mesh	1.003	0.617	1.620
Shell FEA[13]		1.066	0.623	1.680
Plane Strain FEA[13]		1.071	0.658	1.729
	Low Cohesive Stiffness	0.95	0.688	1.638
HyperSizer	Moderate Cohesive Stiffness	0.89	0.65	1.54
	High Cohesive Stiffness	0.84	0.64	1.48

B. Isotropic Double Cantilever Beam Specimen Example

This example problem considers an isotopic double cantilever beam (DCB) fracture specimen that was analyzed by Glaessgen et al.[16] using plane strain and plate FEA models. Note that the nature of the DCB test is such that the crack loading is completely mode I. The problem dimensions are: l = 1 in. and h = 0.025 in. The problem considers an isotropic material with E = 10 Msi and ν = 0.3 and an applied opening shear force resultant (see Fig. 7) of Q = 1 lb/in. As in the previous example problem, the FEA solution of Glaessgen et al.[16] does not include a physical adhesive material, thus the HyperSizer penalty stiffness must be selected. In this case, two penalty stiffness values were considered corresponding to α = 6.25 and α = 62.5 (see equation (9)).

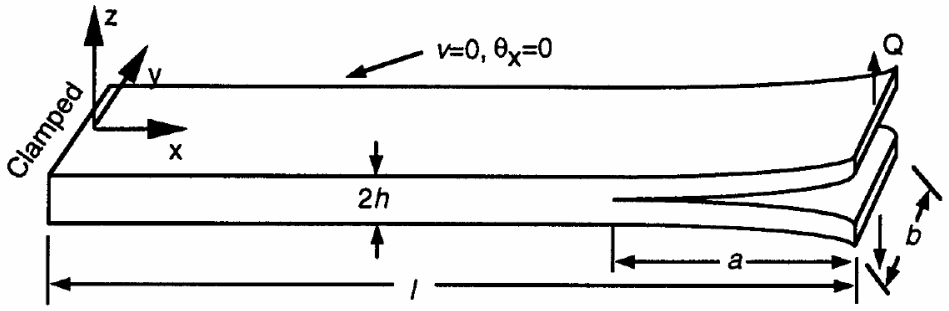

Fig. 7 Double cantilever beam specimen considered by Glaessgen et al.[16], after Glaessgen et al.[16]

Figure 8 shows a plot of the mode I SERR predicted by HyperSizer as a function of crack length for the two cohesive penalty stiffness values, along with the results of Glaessgen et al.[16] for plane strain and plate FEA models. The effect of the penalty stiffness on the HyperSizer predictions decreases with crack size, with a difference of approximately 3% between the two HyperSizer cases at an a/h value of 5. The HyperSizer results agree quite well with the Glaessgen et al.[16] plate FEA results, with the HyperSizer values being somewhat lower for short crack lengths and slightly higher for long cracks. The Glaessgen et al.[16] plane strain FEA results are somewhat higher over most of the crack length range considered.

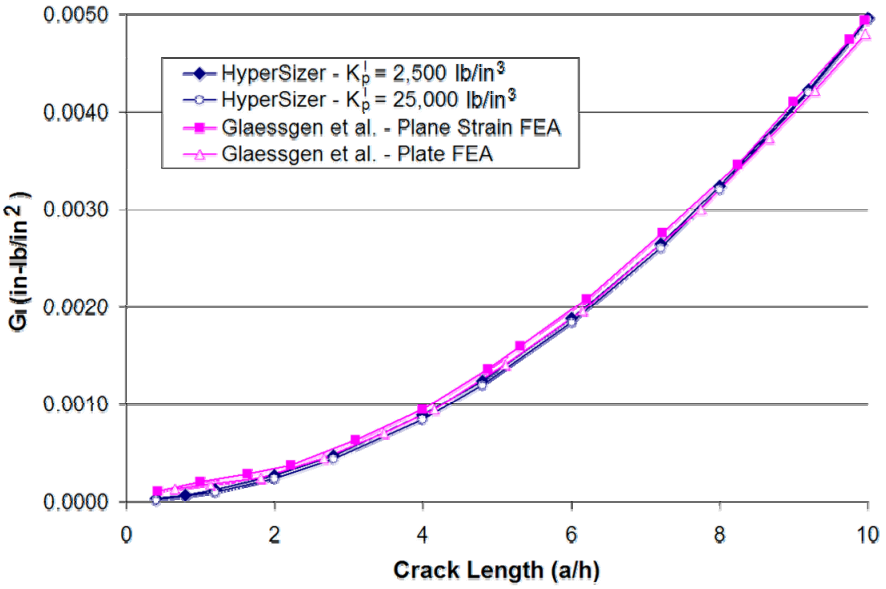

Fig. 8 Comparison of HyperSizer predictions with FEA predictions[16] for the DCB specimen mode I SERR (G_I) as a function of crack length.

C. Orthotropic Double Cantilever Beam Specimen Example

This example problem considers an orthotropic DCB fracture specimen that was analyzed by Crews et al.[17] using a 3D solid FEA model. The problem dimensions are: l = 101.6 mm and t = 1.65 mm; the material properties are: E_1 = 134 GPa, E_2 = 13 GPa, ν_{12} = 0.34, G_{12} = 6.4 GPa, G_{23}= 4.8 GPa; a load of p = 1 N/m is applied. Two mode I cohesive penalty stiffnesses were considered in HyperSizer corresponding to values of α = 3.8 and α = 77 (see equation (9)).

HyperSizer predictions are compared with the results of Crews et al.[17] in Fig. 10 as a function of crack length. It should be noted that the 3D FEA analysis of Crews et al.[17] considered the variation of the SERR along the crack tip front in the y-direction (see Fig. 9), while the HyperSizer joint analysis method contains no such variation. As such, the plot shown in Fig. 10 compares the HyperSizer results with the FEA results averaged over the dimension b (see Fig. 9). The HyperSizer predictions under predict the FEA SERR values to some degree over the range of crack lengths considered, but still match the FEA results reasonably well. The penalty stiffness value had a small but noticeable effect on the HyperSizer results, with the higher penalty stiffness resulting in lower predicted SERR values.

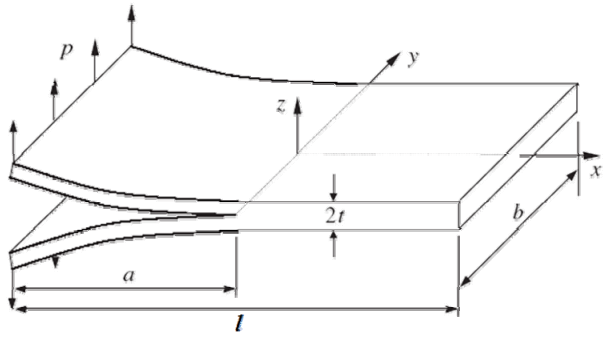

Fig. 9 Double cantilever beam specimen considered by Crews et al.[17], after Zou et al.[18]

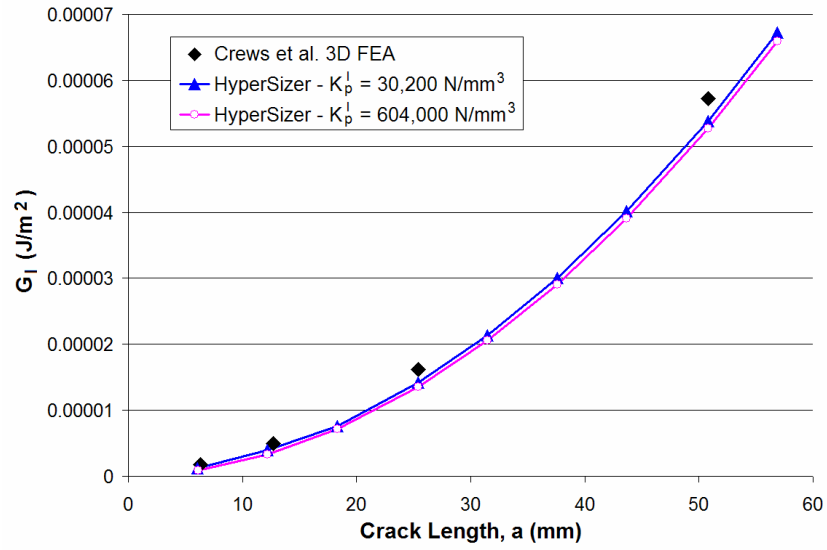

Fig. 10 Comparison of HyperSizer predictions with FEA results[17] for the orthotropic DCB specimen mode I SERR (G_I) as a function of crack length.

D. Mixed Mode Bending Specimen Example

This example considers a graphite/PEEK composite mixed mode bending (MMB) test specimen, shown in Fig. 11. With this test apparatus, by varying the location (c) of the applied load, the mode I to mode II ratio experienced by the specimen can be varied. The dimensions considered in this example problem are: L = 50 mm and h = 3.1 mm; the graphite/PEEK material properties are: E_1 = 116 GPa, E_2 = 10.1 GPa, ν_{12} = 0.329, and G_{12} = 5.5 GPa. The mode I cohesive penalty stiffness employed in the HyperSizer simulations corresponds to value of α = 152 (see equation (9)), while the mode II penalty stiffness was chosen based on an effective cohesive Poisson ratio of 0.3.

Figure 12 compares the HyperSizer predictions for the load point displacement in the MMB specimen example (with c = 41 mm and a = 25 mm) with the experimental and 2D FEA results of Crews and Reeder[19]. These results show excellent agreement between the HyperSizer and experimental results, with the Crews and Reeder[19] FEA results predicting more displacement at a given load. The G_I and G_{II} results reported by Crews and Reeder[19] were normalized to the test load by dividing the SERR by the load point displacement. However, the only load point displacement reported was for the baseline case with a = 25

mm and c = 41 mm, which is shown in Fig. 12. Therefore this is the only case for which a direct comparison of G_I and G_{II} values is possible. This comparison is shown in Table 4. As was the case with the bonded doubler example (see Section IV. A. and Fig. 5), HyperSizer slightly under predicts the G_I value and slightly over predicts the G_{II} value compared to the FEA results, with the total SERR (GT) matching very closely.

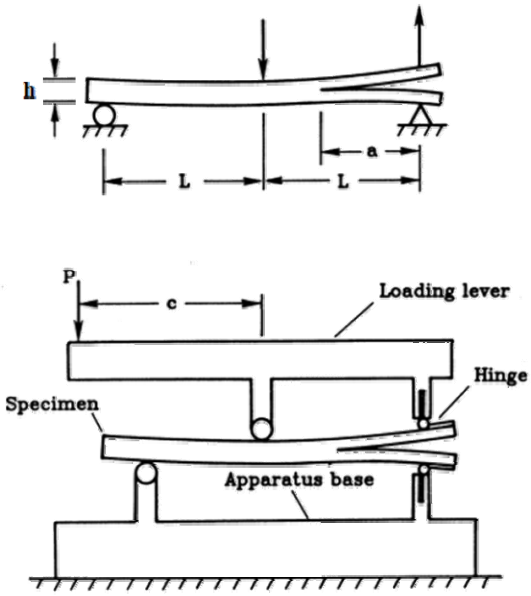

Fig. 11 Mixed mode bending specimen considered by Crews and Reeder[19], after Crews and Reeder[19].

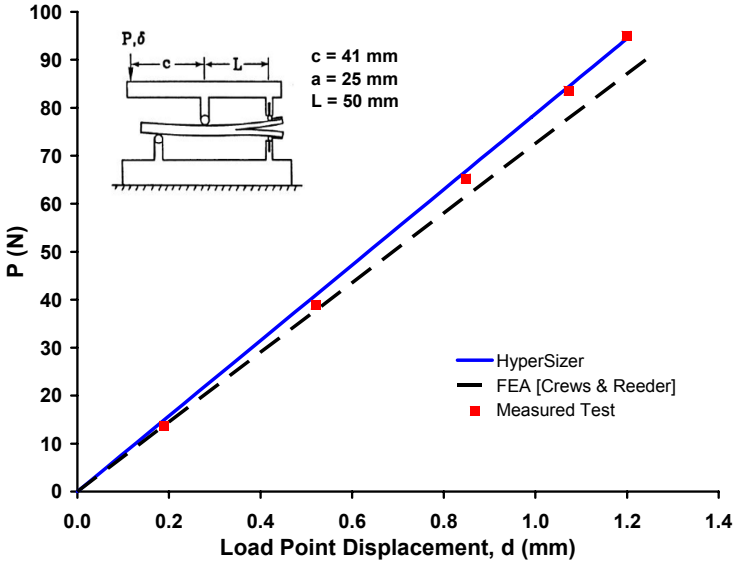

Fig. 12 Comparison of HyperSizer predictions (solid line) of the load point displacement with FEA predictions[19] (dashed line) and test data (points) for the composite MMB specimen.

Table 4 Comparison of HyperSizer SERR predictions of the MMB specimen SERRs with the FEA of Crews and Reeder[19] for the case with c = 41 mm and a = 25 mm (see Fig. 11).

	SERR (J/mm^2)		
	G_I	G_{II}	G_T
FEA[19]	0.0208	.0208	0.0416
HyperSizer	0.0197	.0224	0.0421

As a final comparison, Fig. 13 plots the predicted mode-mixity ratio (G_I/G_{II}) for the MMB example problem as a function of load position (c) for a crack length a = 25 mm. The HyperSizer predictions show reasonably good agreement with the results of the FEA analysis by Crews and Reeder[19]. As would be expected due to the tendency of HyperSizer to under predict G_I and over predict G_{II} compared to FEA, the mode-mixity ratio predicted by HyperSizer is consistently slightly lower than the FEA results.

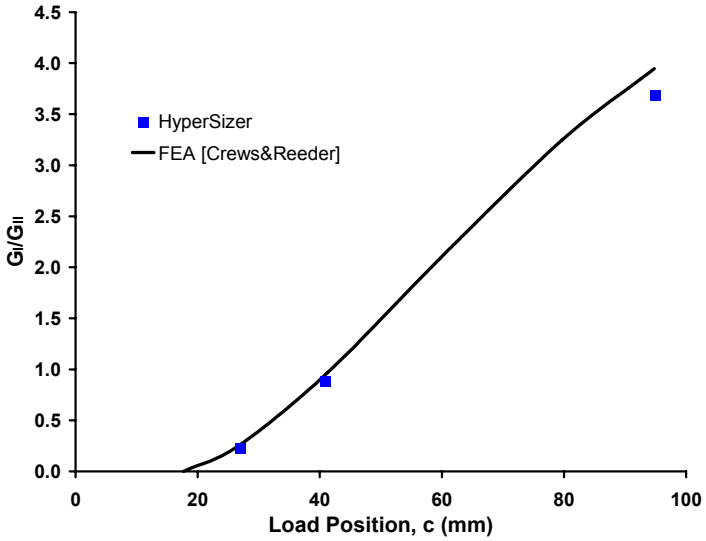

Fig. 13 Comparison of HyperSizer predictions with FEA predictions[19] for the mode-mixity ratio (G_I/G_{II}) of the composite MMB specimen for the case with a = 25 mm (see Fig. 11) as a function of load position (c).

V. Conclusion

The HyperSizer bonded joint analysis capability[1-5], which is based on the efficient, analytical (non-FEA) formulation of Mortensen[8,9], has been extended to include the virtual crack closure technique (VCCT) for predicting crack growth. This has enabled joint design for damage tolerance within the HyperSizer stiffened structural design/analysis/optimization software, with full access to the efficient pre- and post-processing and database functionality of the software. The crack is introduced in the analysis by eliminating cohesion between the adherends at the desired crack location. The mode I, mode II, and mode III strain energy release rates (SERRs) can then be calculated from VCCT similarly to methods used within finite element analysis[7]. This procedure is automated within HyperSizer, with the software

automatically returning SERR values given the joint configuration, loads, material properties, and crack length and location.

Four example problems were presented that serve as validation/verification of the HyperSizer joint analysis VCCT method. These include analyses of a composite bonded doubler joint, isotropic and orthotropic double cantilever beam (DCB) specimens, and a mixed mode bending (MMB) specimen. HyperSizer predictions for these problems were compared with results from the literature that were mainly based on finite element analyses (along with some experimental results for the MMB specimen). In general, the HyperSizer results showed very good agreement with results from the literature.

The effect of analysis point spacing employed within the HyperSizer analysis was also investigated. These points are those at which the solution to the joint governing differential equations is determined, and the convergence of the method SERR predictions with point spacing was illustrated in the presented results. Finally, the effect of the cohesive stiffness between the joint adherends was investigated. Within the HyperSizer joint analysis method, cohesion between the adherends is governed by a traction-separation law that is similar to the linear behavior of cohesive elements with the ABAQUS[10,11] finite element software. When a physical adhesive is present in the joint problem analyzed, this traction-separation law can represent an adhesive material given its elastic moduli (and inelastic behavior) along with its thickness. When no physical adhesive is present, the traction-separation law represents the cohesion between the adherends as a zero-thickness region with a penalty stiffness[11]. It was shown that, while this cohesive penalty stiffness has a large influence on the cohesive stresses, its influence on the predicted SERR values is quite weak. Future work will address this penalty stiffness affect in more detail in pursuit of the most appropriate values to use in the context of HyperSizer joint analysis problems

Acknowledgements This work was partially supported by the Air Force Research Laboratory (AFRL) under contract FA8650-05-M-3527. The authors wish to thank Dr. Steven P. Engelstad of Lockheed Martin Aeronautics Company for suggesting the incorporation of VCCT within HyperSizer and for several fruitful discussions on the subject. We also thank Dr. Carlos P. Davila of NASA Langley and Dr. Stephen B. Clay and Michael A. Falugi of the Air Force Research Laboratory for helpful discussions and support.

References

[1]Zhang, J., Bansal, Y., Bednarcyk, B.A., Collier, C.S., and Pindera, M.-J. "Analysis of Adhesively Bonded Composite Joints Using a Higher-Order Theory" in *Proc. 45th AIAA/ASME/ASCE/AHS/ASC Structures, Structural Dynamics, and Materials Conference*, April, 2004, Palm Springs, California.

[2]Zhang, J., Bednarcyk, B.A., Collier, C., Yarrington, P., Bansal, Y., and Pindera, M.-J., "3D Stress Analysis of Composite Bonded Joints," Proc. *46th AIAA/ASME/ASCE/AHS/ASC Structures, Structural Dynamics, and Materials Conference*, April, 2005, Austin, Texas.

[3]Yarrington, P.W., Zhang, J., Collier, C.S., and Bednarcyk, B.A., "Failure Analysis of Adhesively Bonded Composite Joints" in *Proc. 46th AIAA/ASME/ASCE/AHS/ASC Structures, Structural Dynamics, and Materials Conference*, April, 2005, Austin, Texas.

[4]Bednarcyk, B.A., Zhang, J., Collier, C.S., Bansal, Y., and Pindera, M.-J., "Analysis Tools for Adhesively Bonded Composite Joints, Part I: Higher-Order Theory" *AIAA Journal*, Vol. 44, No. 1, 2006, pp. 171-180.

[5]Zhang, J., Bednarcyk, B.A., Collier, C.S., Yarrington, P.W., Bansal, Y., and Pindera, M.-J., "Analysis Tools for Adhesively Bonded Composite Joints, Part II: Unified Analytical Theory" *AIAA Journal*, In Press.

[6]Rybicki, E.F. and Kanninen, M.F., "A Finite Element Calculation of Stress Intensity Factors by a Modified Crack Closure Integral" *Engineering Fracture Mechanics*, Vol. 9, 1977, pp. 931-938.

[7]Krueger, R. "The Virtual Crack Closure Technique: History, Approach and Applications" *NASA/CR-2002-211628*, April, 2002.

[8]Mortensen, F., "Development of Tools for Engineering Analysis and Design of High-Performance FRP-Composite Structural Elements" Ph.D. Thesis, Institute of Mechanical Engineering, Aalborg University (Denmark), Special Report no. 37, 1998.

[9]Mortensen, F. and Thomsen, O.T., "Analysis of Adhesive Bonded Joints: A Unified Approach," *Composites Science and Technology*, Vol. 62, 2002, pp. 1011-1031.

[10]ABAQUS, Inc., *ABAQUS Analysis User's Manual*, Vol. 4, Version 6.5, 2004.

[11]Camanho, P.P. and Davila, C.G., "Mixed-Mode Decohesion Finite Elements for the Simulation of Delamination in Composite Materials" NASA/TM-2002-211737, 2002.

[12]Davila, C.G., Personal Communication, NASA Langley Research Center, 2006.

[13]Wang, J.T., Raju, I.S., Davila, C.G., and Sleight, D.W., "Computation of Strain Energy Release Rates for Skin-Stiffener Debonds Modeled with Plate Elements" in *Proc. 34th AIAA/ASME/ASCE/AHS/ASC Structures, Structural Dynamics, and Materials Conference*, April, 1993, La Jolla, California, AIAA-93-1501-CP.

[14]Raju, I.S., Sistla, R., and Krishnamurthy, T., "Fracture Mechanics Analyses for Skin-Stiffener Debonding" *Engineering Fracture Mechanics*, Vol. 54, No. 3, 1996, pp. 371-385.

[15]Turon, A., Davila, C.G., Camanho, P.P., and Costa, J., "An Engineering Solution for using Coarse Meshes in the Simulation of Delamination With Cohesive Zone Models" NASA/TM-2005-213547, 2005.

[16]Glaessgen, E.H., Riddell, W.T., and Raju, I.S., "Effect of Shear Deformation and Continuity on Delamination Modeling with Plate Elements" in *Proc. 39th AIAA/ASME/ASCE/AHS/ASC Structures, Structural Dynamics, and Materials Conference*, April, 1998, Long Beach, California, AIAA-1998-2023.

[17]Crews, J.H., Shivakumar, K.N., and Raju, I.S., "Strain Energy Release Rate Distributions for Double Cantilever Beam Specimens" *AIAA Journal*, Vol. 29, No. 10, 1990, pp. 1686-1691.

[18]Zou, Z., Reid, S.R., Li, S., and Soden, P.D., "General Expressions for Energy Release Rates for Delamination in Composite Laminates" *Proceeding of the Royal Society A*, Vol. 458, 2002, pp. 645-667.

[19]Crews, J.H. and Reeder, J.R., "A Mixed-Mode Bending Apparatus for Delamination Testing" NASA/TM-1988-100662, 1988.